Antibacterial Agents Hot Paper

How to cite:
International Edition: doi.org/10.1002/anie.202104024
German Edition: doi.org/10.1002/ange.202104024

Red Light-Triggered Intracellular Carbon Monoxide Release Enables Selective Eradication of MRSA Infection

*Jian Cheng, Guihai Gan, Zhiqiang Shen, Lei Gao, Guoying Zhang, and Jinming Hu**

Abstract: *Carbon monoxide (CO) is an important gaseous signaling molecule. The use of CO-releasing molecules such as metal carbonyls enables the elucidation of the pleiotropic functions of CO. Although metal carbonyls show a broad-spectrum antimicrobial activity, it remains unclear whether the bactericidal property originates from the transition metals or the released CO. Here, we develop nonmetallic CO-releasing micelles via a photooxygenation mechanism of 3-hydroxyflavone derivatives, enabling CO release under red light irradiation (e.g., 650 nm). Unlike metal carbonyls that non-specifically internalize into both Gram-positive and Gram-negative bacteria, the nonmetallic micelles are selectively taken up by S. aureus instead of E. coli cells, exerting a selective bactericidal effect. Further, we demonstrate that the CO-releasing micelles can cure methicillin-resistant S. aureus (MRSA)-infected wounds, simultaneously eradicating MRSA pathogens and accelerating wound healing.*

Introduction

Apart from being an air pollutant, carbon monoxide (CO) is also an endogenous gaseous singling molecule in living organisms,[1] exerting physiological functions such as anti-inflammatory, anti-apoptotic, and anti-cancer effects.[2] Carbon monoxide-releasing molecules (CORMs) such as metal carbonyls are developed for safe and convenient delivery of CO, and these CO-releasing prodrugs render it possible to investigate and understand the physiological functions of CO.[3] Although metal carbonyls provide a robust tool to locally deliver CO and show therapeutic benefits similar to that of CO gas, the use of metal carbonyls to evaluate the antibacterial activity of CO leads to ambiguous conclusions. Specifically, previous studies revealed that the most extensively used CO-releasing metal carbonyls such as CORM-2 (tricarbonyldichlororuthenium(II) dimer) and CORM-3 (tricarbonylchloro(glycinato)ruthenium (II)) showed a broad-spectrum antibacterial activity.[4] However, a saturated solution of CO gas had a negligible effect on inhibiting bacterial growth.[5] Giving that no CO release was detected in biological fluids of CORM-3,[6] these results likely implied that it was the transition metals rather than the released CO exerting the antibacterial effect. Indeed, a recent study concluded that it was the thiol-reactive Ru^{2+} ions instead of CO release that underlined the antibacterial property.[7] Therefore, we surmised that it would be necessary to develop metal-free CO-releasing platforms, which may be beneficial to exclude the influence of metal ions and to clarify the antibacterial capacity of CO.

In the context of nonmetallic CORMs, boranocarbonates,[8] Diels–Alder reaction-based CO donors,[9] and several photoresponsive CORMs (photoCORMs) have been successfully developed.[10] Among them, photoCORMs enabled localized CO delivery by taking advantage of the spatiotemporal precision of light stimulus. Typical nonmetallic photoCORMs include 3-hydroxyflavone (3-HF),[11] cyclic diketone,[12] xanthene-9-carboxylic acid,[13] and *meso*-carboxyl BODIPY derivatives,[14] exhibiting triggered CO release under specific light irradiation (Scheme 1 a). Remarkably, although metal-free photoCORMs have revealed great potentials in anti-inflammatory and anticancer applications,[9b,11c] the antibacterial performance of nonmetallic photoCORMs have far less been explored. Since bacterial pathogens were inherently sensitive to ultraviolet (UV) irradiation, it would be necessary to activate photoCORMs under long-wavelength illumination with decreased phototoxicity. Unfortunately, many of previous photoCORMs were

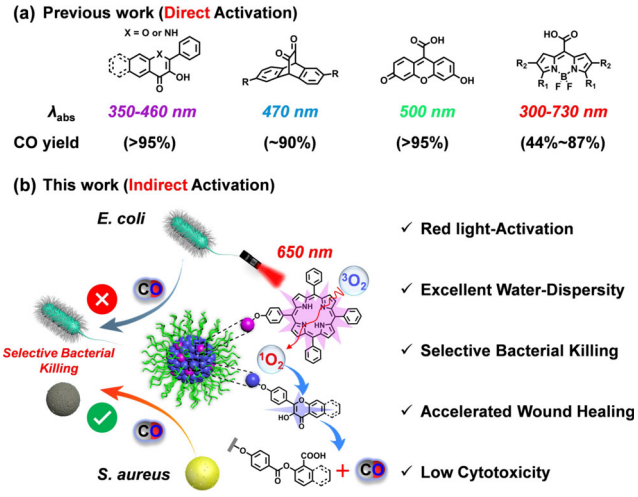

Scheme 1. a) Representative metal-free photoCORMs with typical activation wavelengths and CO yields. b) Illustration of the fabrication of metal-free CO-releasing micelles by integrating 3-HF derivatives and tetraphenylporphyrin (TPP) photosensitizer into the micelle cores, enabling CO release under red light irradiation via a photooxygenation mechanism, exerting a selective bactericidal effect toward Gram-positive bacteria.

[*] J. Cheng, G. Gan, Z. Shen, L. Gao, Prof. Dr. G. Zhang, Prof. Dr. J. Hu
CAS Key Laboratory of Soft Matter Chemistry
Hefei National Laboratory for Physical Science at the Microscale
Department of Polymer Science and Engineering
University of Science and Technology of China
Hefei 230026, Anhui (China)
E-mail: jmhu@ustc.edu.cn
Supporting information and the ORCID identification number(s) for the author(s) of this article can be found under: https://doi.org/10.1002/anie.202104024.

primarily activated by detrimental UV or near-UV light with poor tissue penetration,[15] and it remained a grand challenge to develop photoCORMs capable of releasing CO under red or near-infrared light irradiation.[16] Considering the facile preparation, quantitative CO yield, and low toxicity of the photolyzed products of 3-HF-based CO releasers, we envisioned that 3-HF derivative might be an ideal candidate for metal-free CORMs to evaluate the antibacterial capacity of CO. Nevertheless, it was impractical to directly activate 3-HF moieties under red light irradiation owing to the weak absorbance. It was worth noting that the CO release from 3-HF derivatives involved the oxygenation of excited 3-HF derivatives by ground oxygen ($^3O_2$).[11d] We hypothesized it was possible to oxidize 3-HF derivatives through a photooxygenation mechanism using more oxidative singlet oxygen ($^1O_2$) in the presence of a specific photosensitizer with long-wavelength absorbance, thereby enabling CO release via an indirect approach under red light irradiation.[17]

In this work, we report a metal-free CO-releasing platform by integrating 3-HF derivatives and tetraphenylporphyrin (TPP) moieties into the cores of micellar nanoparticles, serving as the CO donor and photosensitizer, respectively. The formation of micellar nanoparticles not only increased the water-dispersity but also locally concentrated 3-HF derivatives and the photosensitizer. When exposed to 650 nm light irradiation, the excited TPP photosensitizer converted $^3O_2$ to $^1O_2$ that spontaneously oxidized 3-HF derivatives, resulting in CO release (Scheme 1b). The CO-releasing micelles were selectively internalized by Gram-positive *Staphylococcus aureus* (*S. aureus*) instead of Gram-negative *Escherichia coli* (*E. coli*) bacteria, and the red light-triggered intracellular CO release exerted an excellent bactericidal effect against *S. aureus.* Moreover, in vivo studies revealed that the CO-releasing micelles could efficiently eradicate methicillin-resistant *S. aureus* (MRSA) bacteria and accelerate MRSA-infected wounds in a full-thickness skin wound model.

Results and Discussion

Starting from 4-hydroxybenzaldehyde, both 3-HF-based monomers, *N*-(2-(4-(3-hydroxy-4-oxo-4*H*-chromen-2-yl)phenoxy) ethyl)methacrylamide (HFM) and *N*-(2-(4-(3-hydroxy-4-oxo-4*H*-benzo[g]chromen-2-yl)phenoxy)ethyl)methacrylamide (FlavM), were successfully synthesized using a similar procedure. Moreover, the phenolic group of HFM could be further modified with the formation of caged HF monomer (CHFM) in the presence of benzyl bromide (Supporting Information, Scheme S1). Also, we synthesized TPP photosensitizer-based monomer (TPPM; Scheme S2) and HF, TPP-HF, TPP-CHF, and TPP-Flav block copolymers through reversible addition-fragmentation chain transfer (RAFT) polymerization (Scheme S3).[18] All the precursors, targeted monomers, and block copolymers were thoroughly characterized (Figures S1–S11). The chemical structures and the structural parameters of the as-synthesized diblock copolymers are shown in Scheme 2 and Table S1, respectively. Remarkably, although phenol-containing compounds were known as inhibitors of radicals, the HFM and FlavM monomer containing a phenolic group at the 3-position could be directly polymerized through RAFT polymerization.

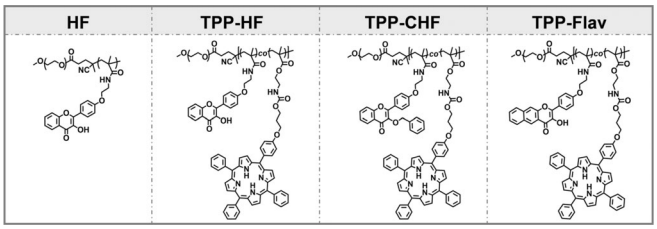

Scheme 2. Chemical structures of HF, TPP-HF, TPP-CHF, and TPP-Flav diblock copolymers used in this study.

With the synthesized block copolymers in hand, we first investigated their self-assembly behavior in aqueous solutions. TPP-HF, TPP-CHF, and HF block copolymers self-assembled into micellar nanoparticles with hydrodynamic diameters, $\langle D_h \rangle$, of ca. 20–60 nm (Figure S12). Upon exposure to mild red light irradiation (650 nm, 26 mW cm^{-2}), no significant changes in $\langle D_h \rangle$ were observed for all three micelles, whereas a decrease in scattering intensities was observed for TPP-HF micelles (Figure 1a–c, S12). To understand this phenomenon, we monitored the UV/Vis absorbance spectra of all three micelles under 650 nm light irradiation. We found that a continuous decrease centered at 356 nm was only observed for TPP-HF micelles (Figure 1d), whereas TPP-CHF micelles with caged 3-HF moieties and HF micelles without the labeling of TPP photosensitizers did not reveal noticeable changes in UV/Vis spectra (Figure S13). The apparent photolysis constant, k_{obs}, of TPP-HF micelles was determined to be 0.08 min^{-1} under 650 nm light irradiation (Figure S13d and Table S2). Remarkably, when TPP-HF micelles were exposed to 365 nm light irradiation, the k_{obs} value was increased to 0.151 min^{-1} (Figure S14), which was likely ascribed to the higher absorbance at 365 nm (Figure 1d). However, the k_{obs} of HF micelles without TPP photosensitizer dropped to 0.034 min^{-1} under identical 365 nm light irradiation (Figure S14 and Table S2), demonstrating that the photolysis of 3-HF moieties proceeded more efficiently in the presence of TPP photosensitizer under 650 nm light irradiation.

Using the allyl-Flu (AFCO) probe,[19] red light-mediated CO release from TPP-HF micelles was confirmed by the fluorescence increase (Figure 1e). Moreover, the CO release process was monitored by a portable CO detector (Dräger Pac6500), revealing that a higher CO yield under 650 nm irradiation than that of 365 nm irradiation (Figure 1f). Specifically, the CO release amounts were calculated to be 1.26 μmol and 1.06 μmol under 650 and 365 nm irradiation for 90 min, corresponding to ca. 69% and ca. 58% of the 3-HF moieties, respectively (Figure 1f). However, no CO release was detected for TPP-CHF and HF micelles under identical red light irradiation (Figure 1f), in good agreement with the negligible changes in UV/Vis spectra (Figure 1d and S13). Taken together, although 3-HF moieties showed negligible absorbance at 650 nm, the incorporation of TPP photosensitizer and 3-HF moieties into the cores of micellar nanoparticles enabled the photooxygenation of 3-HF moieties,

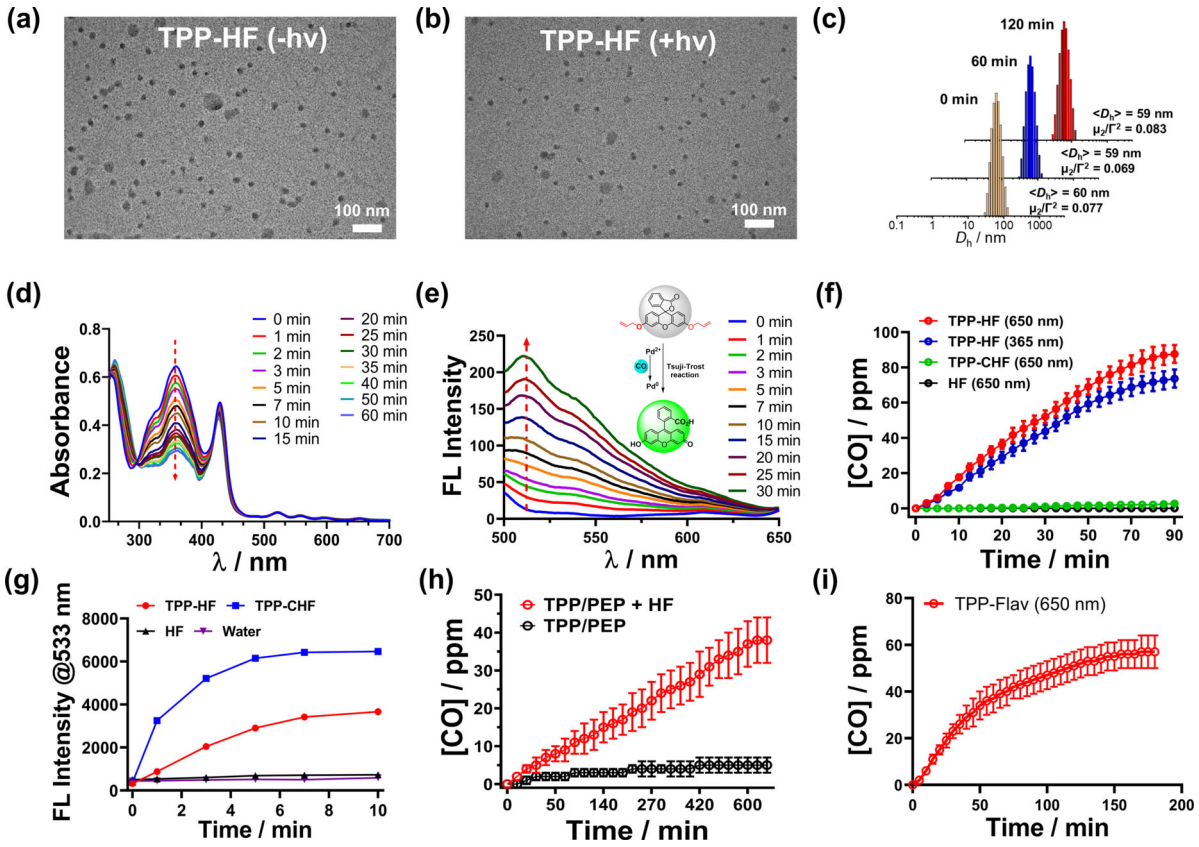

Figure 1. a),b) TEM images and c) intensity-average hydrodynamic diameter distributions of TPP-HF micelles with 650 nm irradiation for 0–120 min. d) UV/Vis spectra of TPP-HF micelles (0.1 g L^{-1}) under 650 nm irradiation. e) Evolution of fluorescence emission spectra (λ_{ex} = 490 nm) of TPP-HF micelles with allyl-Flu probe (AFCO; 5 μM) and $PdCl_2$ (5 μM) under 650 nm irradiation. f) CO release profiles of TPP-HF, TPP-CHF, and HF micelles (0.1 g L^{-1}) in PBS under varying irradiation conditions (650 nm, 26 mW cm^{-2} or 365 nm, 6.8 mW cm^{-2}). g) Fluorescence intensity of SOSG at 533 nm in the presence of TPP-HF, TPP-HF, and HF micelles (0.1 g L^{-1}) with 650 nm irradiation (26 mW cm^{-2}). h) CO release profiles of DMF solution of HF (0.2 mg mL^{-1}) in the presence of pre-irradiated PEP (1.0 mg mL^{-1}) under dark condition. Pre-treated PEP was irradiated with 650 nm light for 60 min in the presence of TPPM (0.2 mg mL^{-1}). i) CO release profiles of TPP-Flav micelles (0.1 g L^{-1}) in PBS under 650 nm irradiation. In all cases, the irradiation intensity was 26 mW cm^{-2}.

resulting in CO release under red light irradiation. It should be mentioned that the control experiments revealed that the coexistence of free phenolic group and TPP photosensitizer was indispensable to enable the 3-HF derivatives to be activated by red light irradiation because neither TPP-CHF with caged 3-HF moieties nor HF micelles without TPP photosensitizer could release CO under otherwise identical conditions.

To clarify the CO release mechanism under red light irradiation, we deoxygenated the TPP-HF micelles by three freeze-pump-thaw cycles and exposed the degassed micelles to the same light source. There were no remarkable changes in the UV/Vis spectra (Figure S15), implying the involvement of oxygen in the photolysis process. Moreover, the generation of $^1O_2$ under 650 nm light irradiation was observed for both TPP-HF and TPP-CHF micelles, as probed by $^1O_2$-specific Singlet Oxygen Sensor Green (SOSG). The fluorescence intensity of SOSG was stronger for TPP-CHF than that of TPP-HF micelles with a similar TPP concentration, which was tentatively ascribed to the consumption of $^1O_2$ by 3-HF moieties (Figure 1g and S16). By contrast, no $^1O_2$ was detected for HF micelles without TPP photosensitizer (Figure 1g). These results corroborated the involvement of oxygen in the photolysis process. To further support this claim, we synthesized PYD diblock copolymer capable of capturing and releasing $^1O_2$. The conversion of pyridone to endoperoxide moieties under 650 nm light irradiation in the presence of TPP photosensitizer was monitored by UV/Vis spectra. The formation of $^1O_2$-releasing endoperoxide-containing PEP diblock copolymers was evidenced by the absorbance decrease at 302 nm (Figure S17).[20] Upon incubation of HF micelles with PEP block copolymers, spontaneous CO release was detected again even under dark conditions (Figure 1h). In addition, we found that TPP-Flav micelles with extended 3-HF moieties underwent red light-triggered CO release as well, suggesting a general procedure for the activation of 3-HF derivatives (Figure 1i). Also, we analyzed the photolyzed product of HFM monomer in the presence of TPP photosensitizer under 650 nm light irradiation, revealing the formation of 2-(benzoyloxy)benzoic acid derivatives by HRMS (Figure S18), which was identical to the photolyzed product under UV light irradiation.[11e] Building on the above results, we surmised that, under 650 nm light irradiation, the excited TPP photosensitizer produced $^1O_2$

within micellar nanoparticles, which in turn oxidized the 3-HF moieties in close proximity within the cores, thereby triggering CO release under red light irradiation. Moreover, the photooxidation process under red light irradiation (e.g., 650 nm) gave rise to more efficient CO release in terms of faster release kinetic and higher CO yield, which was quite beneficial for potential biomedical applications with decreased phototoxicity and increased CO production.

Next, we investigated whether the CO-releasing micelles had an antimicrobial capacity. Although irradiation of Gram-positive *S. aureus* bacteria with 650 nm (26 mW cm^{-2}) did not affect the bacterial viability within 30 min (Figure 2a), we found that the viability of *S. aureus* bacteria drastically decreased (ca. 92%) after 10 min irradiation in the presence of TPP-HF micelles, and no bacterial colonies were observed after 20 min irradiation (Figure 2a). Notably, although HF block copolymer could release CO under 365 nm irradiation (Figure 1f), we found that both *S. aureus* and *E. coli* cells were sensitive to 365 nm irradiation even at a very low light intensity (e.g., 2.2 mW cm^{-2}) for 20 min (Figure S19), which was unfavorable for examining the antibacterial capacity of CO due to the inherent phototoxicity. As such, the current photooxidation strategy enabling CO release under 650 nm irradiation was quite advantageous to evaluate the antimicrobial performance of CO due to decreased phototoxicity.

Notably, although TPP-CHF micelles produced cytotoxic $^1O_2$ (Figure 1g), there was no appreciable bacterial death after 10 min irradiation and only a mild decrease (ca. 20%) in cell viability after 30 min irradiation (Figure 2a). Although $^1O_2$ has been extensively used for bacterial killing,[21] the compromised bactericidal effect of TPP-CHF was likely due to the short working distance of $^1O_2$ (e.g., ca. 10–20 nm). The generated $^1O_2$ had to diffuse out from the inner cores of TPP-CHF micelles (ca. 60 nm in diameter, Figure S12) before taking any action on bacterial killing,[22] which may surpass the working distance of $^1O_2$. Therefore, the micelle formulation was advantageous not only for the photooxidation of 3-HF moieties within micellar cores but also for minimizing the interferences of $^1O_2$. Notably, no antimicrobial capacity was observed for HF micelles that released neither CO nor $^1O_2$ under 650 nm light irradiation (Figure 1g). Moreover, TPP-HF micelles showed a concentration-dependent bactericidal performance under 650 nm light irradiation. Impressively, at a micelle concentration of 0.025 g L^{-1}, ca. 98% bacteria were killed after 30 min irradiation, showing an excellent antimicrobial performance of TPP-HF micelles (Figure 2b). By sharp contrast, none of TPP-HF, TPP-CHF, or HF micelles led to statistically significant decreases in bacterial viability of *E. coli* after 650 nm irradiation for 30 min (Figure 2c,d). These results demonstrated that the CO-releasing micelles exerted a selective antimicrobial property toward *S. aureus* bacteria. However, previous studies revealed a broad-spectrum bactericidal effect of metal carbonyls toward both Gram-positive and Gram-negative bacteria.[4a,d]

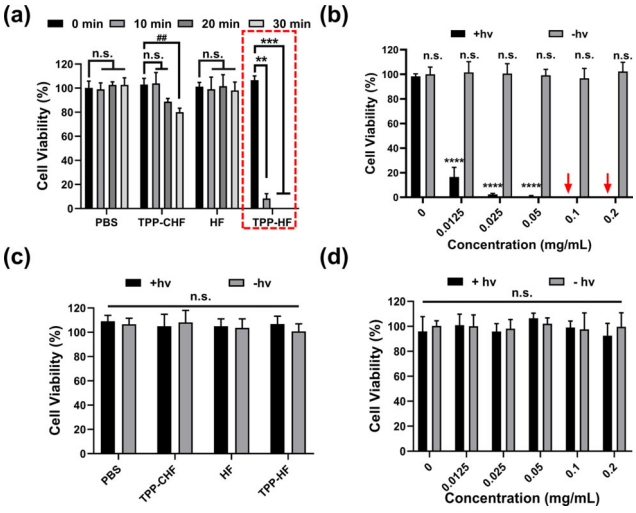

Figure 2. a) Irradiation time-dependent bacterial viability of *S.aureus* after treatment with TPP-CHF, HF, and TPP-HF micelles (0.1 g L^{-1}) with 650 nm light irradiation (26 mW cm^{-2}) for 0–30 min, respectively. $^{\#\#}$ $p<0.01$, in comparison with the non-irradiated group; ** $p<0.01$, *** $p<0.001$, in comparison with the non-irradiated group; n.s., not significant. b) Bacterial viability of *S.aureus* in the presence of varying concentrations of TPP-HF micelles with or without 650 nm light irradiation 30 min (26 mW cm^{-2}). *** $p<0.001$, **** $p<0.0001$, n. s. not significant, in comparison with the PBS group with irradiation. c) *E. coli* viability in the presence of TPP-CHF, HF, and TPP-HF micelles (0.1 g L^{-1}) with or without 650 nm light irradiation (26 mW cm^{-2}) for 30 min. n.s., not significant. d) Bacterial viability of *E. coli* in the presence of varying concentrations of TPP-HF micelles with or without 650 nm light irradiation 30 min (26 mW cm^{-2}). n.s., not significant.

To understand the selective bactericidal effect of TPP-HF micelles toward *S. aureus* cells, we examined the bactericidal performance of pre-irradiated TPP-HF micelles, revealing bacterial killing capacity toward neither *S. aureus* nor *E. coli* (Figure S20). This result likely suggested that photo-triggered CO release was crucial for the antibacterial performance. However, we found that the incubation of *S. aureus* and *E. coli* cells in saturated CO solution (ca. 1 mM; much higher than that of the release CO contents) for 30 min did not induce bacterial death, regardless of 650 nm light irradiation (Figure S21), in line with previous results.[5] The contradictory results revealed that the localized delivery of CO produced distinct antibacterial outcomes in comparison with direct CO administration. A similar phenomenon was also observed for the discrepant antimicrobial performance between CO gas solution and CO-releasing metal carbonyls.[4b,f,g]

Previous results demonstrated that the antimicrobial effects of metal carbonyls primarily originated from the accumulated metal ions in cells rather than released CO.[4b,7] We then evaluated the bacterial internalization performance of CO-releasing micellar nanoparticles. Zeta-potential measurements revealed that TPP-HF, TPP-CHF, and HF micelles were negatively charged with zeta potentials of −32, −21, and −26 mV, respectively (Figure S22a). Upon incubation of both *S. aureus* and *E. coli* bacteria with micellar nanoparticles, no significant changes in zeta potentials were observed either (Figure S22b). This was in sharp contrast to cationic polymer-based antibacterial agents that exerted an antibacterial activity by disrupting bacterial membranes through electrostatic interaction between negatively charged bacterial membranes and positively charged polymers.[23] Interestingly, albeit negatively charged, we found that TPP-HF micelles

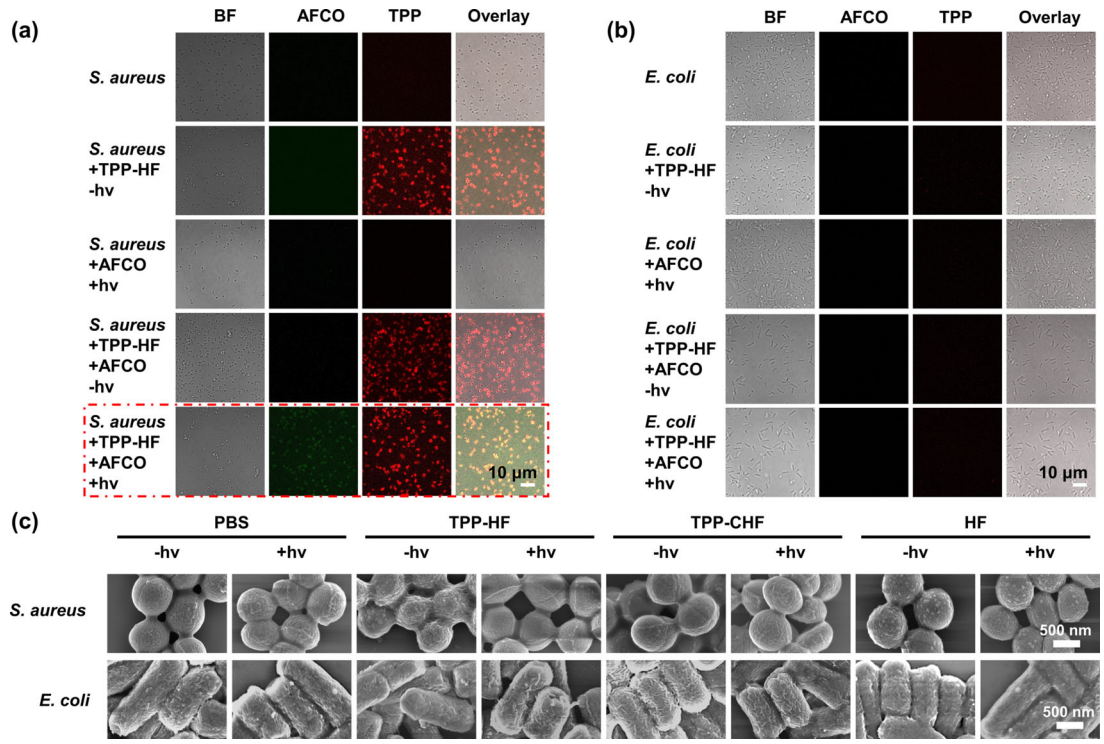

Figure 3. CLSM images of a) *S. aureus* and b) *E. coli* bacteria incubated with TPP-HF (0.1 $g L^{-1}$) under varying conditions. The green channel was excited at 488 nm and collected at 500–600 nm. The red channel was excited at 594 nm and collected at 630–700 nm. c) SEM images of *S. aureus* and *E. coli* cells in the presence of TPP-HF, TPP-CHF, or HF micelles with or without 650 nm light irradiation for 30 min.

could be selectively taken up by *S. aureus*, as evidenced by the appearance of red fluorescence of TPP moieties within *S. aureus* cells. Moreover, red light-triggered CO release within *S. aureus* cells could be detected by the CO-specific AFCO probe as well (Figure 3a).[19] Nevertheless, TPP-HF micelles cannot be internalized into *E. coli* cells and no intracellular CO release was detected (Figure 3b). The different bacterial uptake performance was likely due to the distinct membrane structures of *S. aureus* and *E. coli* cells.[24] Scanning electron microscopy (SEM) revealed no remarkable changes in cell morphologies for both *S. aureus* and *E. coli* (Figure 3c), demonstrating that the selective bacterial killing performance was not ascribed to the disruption of cellular membranes, in agreement with the negatively charged nature of micellar nanoparticles. Therefore, we concluded that the localized CO release within *S. aureus* bacteria played a crucial role in bacterial killing, while the detailed antimicrobial mechanism needs to be further elucidated. Remarkably, the discriminative antibacterial capacity is advantageous for inhibiting the development of drug resistance in bacteria.[25]

Giving that CO-releasing TPP-HF micelles can selectively kill *S. aureus* cells under red light irradiation, we further investigated the CO-releasing micelles for the treatment of methicillin-resistant *S. aureus* (MRSA) infection in a full-thickness skin wound model by taking advantage of the multiple roles of CO in terms of bacterial eradication and accelerating wound healing.[3] MRSA serves as the main reason for skin infections and it may cause pneumonia and other severe diseases, representing a huge threat to human health.[26] In vitro antibacterial assay revealed that TPP-HF micelles (0.1 $g L^{-1}$) eradicated ca. 97% MRSA cells after 30 min irradiation, whereas neither TPP-CHF nor HF under otherwise identical conditions gave rise to statistically significant decreases in bacterial viability (Figure S23). Therefore, CO-releasing TPP-HF micelles could be potentially used for the treatment of MRSA infection.

Next, skin wounds (ca. 5 mm in diameter) were made by a surgical blade and the wounds were inoculated with MRSA cells.[27] After 6 h of infection, the infected wounds were then treated with PBS (negative control), vancomycin (positive control), and TPP-CHF and TPP-HF micelles with or without 650 nm irradiation (Figure 4a). HF micelles released neither CO nor $^1O_2$ were excluded for in vivo antibacterial evaluation (Figure 2). The wounds were treated with 25 μL of micelles following light irradiation (650 nm, 30 min) once per day and the infected areas were continuously monitored within 9 days post-treatment. Notably, the wounds of the TPP-HF micelle-treated group with irradiation completely healed after 9 days, whereas other groups including vancomycin-treated one showed unhealed wounds (Figure 4b,c). Moreover, the bacterial amounts on days 1, 3, and 5 post-treatment were checked by standard colony-forming unit (cfu) count, revealing the least bacterial burden for TPP-HF micelle-treated group (Figures 4d,e and S24), in good agreement with the faster wound healing performance (Figure 4b,c). In vitro scratch assay further supported that the red light-triggered CO release from TPP-HF micelles boosted the wound healing (Figure S25), likely due to the inherent property of CO on accelerating wound healing. Hematoxylin and eosin (H&E)- and Sirius red-staining and CD31-immunostaining analysis

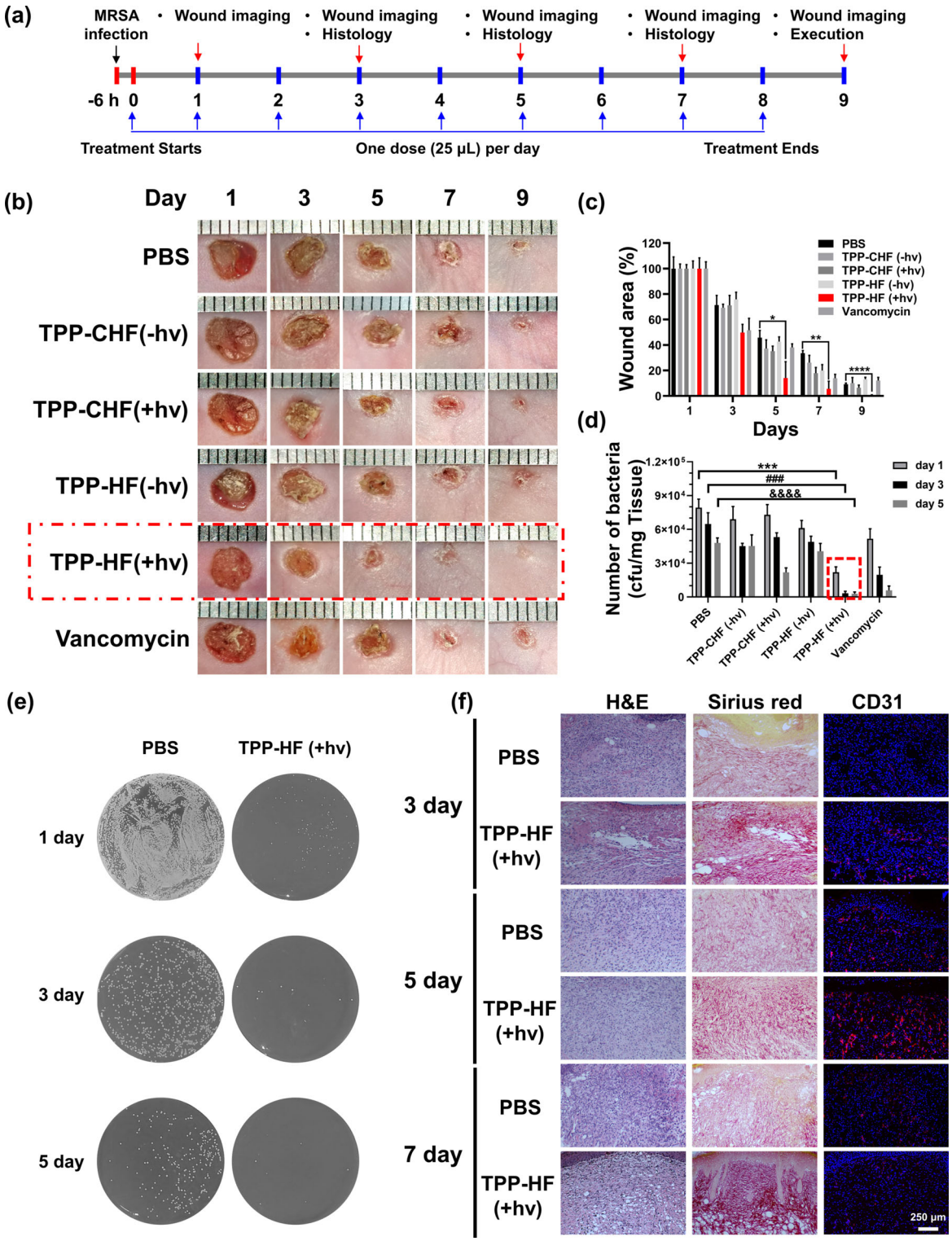

Figure 4. a) Experimental outline of in vivo antibacterial assessment in an MRSA-infected wound healing model. b) Representative skin wound images at 1, 3, 5, 7, 9 days and c) Quantitative analysis of the residual wounded areas receiving different treatments (PBS, TPP-HF(-hv), TPP-HF(+hv), TPP-CHF(-hv), TPP-CHF(+hv), and vancomycin). *, $p<0.05$, **$p<0.01$, **** $p<0.0001$, compared with PBS group. d) Bacterial colony-forming units obtained from different tissues of mice with varying treatments.***, $p<0.001$, $^{###}$, $p<0.001$, $^{\&\&\&\&}$, $p<0.0001$, compared with PBS groups on days 1, 3, 5, respectively. e) Photographs of bacterial colonies on the agar plates of the wounded tissues receiving PBS and TPP-HF (+hv) treatments. f) Histologic analysis of the MRSA-infected wounds receiving different treatments. The scale bar is 250 μm.

revealed that TPP-HF micelles remarkably decreased the infiltration of inflammatory cells, facilitating angiogenesis and collagen deposition, showing better antibacterial and wound healing performance than that of vancomycin and other

control groups (Figure 4 f and S26). Besides, cell viability test against normal mammalian cells (using mouse fibroblast L929 cells as an example) revealed that none of TPP-HF, TPP-CHF, and HF micelles showed obvious toxicity at a micelle concentration of 0.1 $g\,L^{-1}$ (Figure S27). Moreover, hemolysis assay demonstrated that the negatively charged TPP-HF, TPP-CHF, and HF micelles did not lead to detectable hemolysis either, regardless of 650 nm light irradiation (Figure S28). Therefore, the nonmetallic CO-releasing micelles may provide an alternative strategy to combat MRSA infection with low toxicity and hemolysis toward normal cells.

Conclusion

We have successfully developed a new strategy to activate CO-releasing 3-HF moieties through a photooxygenation mechanism, enabling CO release under red light irradiation. This nonmetallic CO-releasing micelle eliminates the interference of transition metal ions, representing an ideal tool to evaluate the antibacterial capacity of CO. Our results suggested that the CO-releasing micelles could be selectively taken up by *S. aureus* rather than *E. coli* cells, enabling intracellular CO release under red light irradiation and exerting a selective antimicrobial effect toward only *S. aureus* bacteria. In vivo study revealed that the CO-releasing micelles could be used for both eradicating MRSA pathogens and accelerating MRSA-infected wound healing. This work not only provides a new strategy to activate photoCORMs but also sheds light on the crucial role of intracellular CO delivery on antibacterial capacity.

Acknowledgements

The financial supports of the National Key R&D Program of China (2020YFA0710700), the National Natural Scientific Foundation of China (NNSFC) Projects (51690150, 51690154, 52073270, 51722307, and 51973206), and the Fundamental Research Funds for the Central Universities (WK2060190102) is gratefully acknowledged.

Conflict of interest

The authors declare no conflict of interest.

Keywords: antibacterial agents · carbon monoxide · MRSA · photooxidation · wound healing

[1] A. Verma, D. J. Hirsch, C. E. Glatt, G. V. Ronnett, S. H. Snyder, *Science* **1993**, *259*, 381 – 384.

[2] a) C. C. Romão, W. A. Blättler, J. D. Seixas, G. J. L. Bernardes, *Chem. Soc. Rev.* **2012**, *41*, 3571 – 3583; b) S. García-Gallego, G. J. L. Bernardes, *Angew. Chem. Int. Ed.* **2014**, *53*, 9712 – 9721; *Angew. Chem.* **2014**, *126*, 9868 – 9877; c) U. Hasegawa, A. J. van der Vlies, E. Simeoni, C. Wandrey, J. A. Hubbell, *J. Am. Chem. Soc.* **2010**, *132*, 18273 – 18280; d) L. E. Otterbein, F. H. Bach, J. Alam, M. Soares, H. T. Lu, M. Wysk, R. J. Davis, R. A. Flavell, A. M. K. Choi, *Nat. Med.* **2000**, *6*, 422 – 428; e) S. Y. Tao, J. Cheng, G. Su, D. Li, Z. Q. Shen, F. H. Tao, T. You, J. M. Hu, *Angew. Chem. Int. Ed.* **2020**, *59*, 21864 – 21869; *Angew. Chem.* **2020**, *132*, 22048 – 22053; f) J. Cheng, B. Zheng, S. Cheng, G. Y. Zhang, J. M. Hu, *Chem. Sci.* **2020**, *11*, 4499 – 4507; g) K. M. Dillon, R. J. Carrazzone, J. B. Matson, K. Kashfi, *Biochem. Pharmacol.* **2020**, *176*, 113931.

[3] R. Motterlini, L. E. Otterbein, *Nat. Rev. Drug Discovery* **2010**, *9*, 728-U724.

[4] a) L. S. Nobre, J. D. Seixas, C. C. Romao, L. M. Saraiva, *Antimicrob. Agents Chemother.* **2007**, *51*, 4303 – 4307; b) S. McLean, R. Begg, H. E. Jesse, B. E. Mann, G. Sanguinetti, R. K. Poole, *Antioxid. Redox Signaling* **2013**, *19*, 1999 – 2012; c) M. Klinger-Strobel, S. Glaser, O. Makarewicz, R. Wyrwa, J. Weisser, M. W. Pletz, A. Schiller, *Antimicrob. Agents Chemother.* **2016**, *60*, 4037 – 4046; d) K. S. Davidge, G. Sanguinetti, C. H. Yee, A. G. Cox, C. W. McLeod, C. E. Monk, B. E. Mann, R. Motterlini, R. K. Poole, *J. Biol. Chem.* **2009**, *284*, 4516 – 4524; e) D. Nguyen, T. K. Nguyen, S. A. Rice, C. Boyer, *Biomacromolecules* **2015**, *16*, 2776 – 2786; f) J. L. Wilson, H. E. Jesse, B. Hughes, V. Lund, K. Naylor, K. S. Davidge, G. M. Cook, B. E. Mann, R. K. Poole, *Antioxid. Redox Signaling* **2013**, *19*, 497 – 509; g) M. Desmard, R. Foresti, D. Morin, M. Dagoussat, A. Berdeaux, E. Denamur, S. H. Crook, B. E. Mann, D. Scapens, P. Montravers, J. Boczkowski, R. Motterlini, *Antioxid. Redox Signaling* **2012**, *16*, 153 – 163; h) J. S. Ward, J. M. Lynam, J. Moir, I. J. S. Fairlamb, *Chem. Eur. J.* **2014**, *20*, 15061 – 15068; i) C. S. Bang, R. Kruse, K. Johansson, K. Persson, *BMC Microbiol.* **2016**, *16*, 64.

[5] L. K. Wareham, R. K. Poole, M. Tinajero-Trejo, *J. Biol. Chem.* **2015**, *290*, 18999 – 19007.

[6] T. Santos-Silva, A. Mukhopadhyay, J. D. Seixas, G. J. L. Bernardes, C. C. Romao, M. J. Romao, *J. Am. Chem. Soc.* **2011**, *133*, 1192 – 1195.

[7] H. M. Southam, T. W. Smith, R. L. Lyon, C. Liao, C. R. Trevitt, L. A. Middlemiss, F. L. Cox, J. A. Chapman, S. F. El-Khamisy, M. Hippler, M. P. Williamson, P. J. F. Henderson, R. K. Poole, *Redox Biol.* **2018**, *18*, 114 – 123.

[8] R. Alberto, K. Ortner, N. Wheatley, R. Schibli, A. P. Schubiger, *J. Am. Chem. Soc.* **2001**, *123*, 3135 – 3136.

[9] a) X. Y. Ji, K. Damera, Y. Q. Zheng, B. C. Yu, L. E. Otterbein, B. H. Wang, *J. Pharm. Sci.* **2016**, *105*, 406 – 416; b) Y. Q. Zheng, X. Y. Ji, B. C. Yu, K. L. Ji, D. Gallo, E. Csizmadia, M. Y. Zhu, M. R. Choudhury, L. K. C. De La Cruz, V. Chittavong, Z. X. Pan, Z. N. Yuan, L. E. Otterbein, B. H. Wang, *Nat. Chem.* **2018**, *10*, 787 – 794.

[10] a) N. Abeyrathna, K. Washington, C. Bashur, Y. Liao, *Org. Biomol. Chem.* **2017**, *15*, 8692 – 8699; b) L. Štacková, M. Russo, L. Muchová, V. Orel, L. Vítek, P. Štacko, P. Klán, *Chem. Eur. J.* **2020**, *26*, 13184 – 13190.

[11] a) L. S. Lazarus, A. D. Benninghoff, L. M. Berreau, *Acc. Chem. Res.* **2020**, *53*, 2273 – 2285; b) Y. Li, Y. Z. Shu, M. W. Liang, X. L. Xie, X. Y. Jiao, X. Wang, B. Tang, *Angew. Chem. Int. Ed.* **2018**, *57*, 12415 – 12419; *Angew. Chem.* **2018**, *130*, 12595 – 12599; c) M. Popova, T. Soboleva, S. Ayad, A. D. Benninghoff, L. M. Berreau, *J. Am. Chem. Soc.* **2018**, *140*, 9721 – 9729; d) S. N. Anderson, J. M. Richards, H. J. Esquer, A. D. Benninghoff, A. M. Arif, L. M. Berreau, *ChemistryOpen* **2015**, *4*, 590 – 594; e) T. Soboleva, H. J. Esquer, A. D. Benninghoff, L. M. Berreau, *J. Am. Chem. Soc.* **2017**, *139*, 9435 – 9438.

[12] P. Peng, C. M. Wang, Z. Shi, V. K. Johns, L. Y. Ma, J. Oyer, A. Copik, R. Igarashi, Y. Liao, *Org. Biomol. Chem.* **2013**, *11*, 6671 – 6674.

[13] L. A. P. Antony, T. Slanina, P. Sebej, T. Solomek, P. Klan, *Org. Lett.* **2013**, *15*, 4552 – 4555.

[14] E. Palao, T. Slanina, L. Muchova, T. Solomek, L. Vitek, P. Klan, *J. Am. Chem. Soc.* **2016**, *138*, 126 – 133.

[15] A. Lipovsky, Y. Nitzan, A. Gedanken, R. Lubart, *Lasers Surg. Med.* **2010**, *42*, 467 – 472.
[16] S. H. C. Askes, G. U. Reddy, R. Wyrwa, S. Bonnet, A. Schiller, *J. Am. Chem. Soc.* **2017**, *139*, 15292 – 15295.
[17] a) S. L. Studer, W. E. Brewer, M. L. Martinez, P. T. Chou, *J. Am. Chem. Soc.* **1989**, *111*, 7643 – 7644; b) M. Russo, P. Stacko, D. Nachtigallova, P. Klan, *J. Org. Chem.* **2020**, *85*, 3527 – 3537.
[18] N. Corrigan, K. Jung, G. Moad, C. J. Hawker, K. Matyjaszewski, C. Boyer, *Prog. Polym. Sci.* **2020**, *111*, 101311.
[19] S. M. Feng, D. D. Liu, W. Y. Feng, G. Q. Feng, *Anal. Chem.* **2017**, *89*, 3754 – 3760.
[20] a) J. H. Zou, J. W. Zhu, Z. Yang, L. Li, W. P. Fan, L. C. He, W. Tang, L. M. Deng, J. Mu, Y. Y. Ma, Y. Y. Cheng, W. Huang, X. C. Dong, X. Y. Chen, *Angew. Chem. Int. Ed.* **2020**, *59*, 8833 – 8838; *Angew. Chem.* **2020**, *132*, 8918 – 8923; b) S. Benz, S. Notzli, J. S. Siegel, D. Eberli, H. J. Jessen, *J. Med. Chem.* **2013**, *56*, 10171 – 10182.
[21] A. Hirao, S. Sato, D. Saitoh, N. Shinomiya, H. Ashida, M. Obara, *Photochem. Photobiol.* **2010**, *86*, 426 – 430.
[22] J. Moan, K. Berg, *Photochem. Photobiol.* **1991**, *53*, 549 – 553.
[23] a) F. Nederberg, Y. Zhang, J. P. K. Tan, K. J. Xu, H. Y. Wang, C. Yang, S. J. Gao, X. D. Guo, K. Fukushima, L. J. Li, J. L. Hedrick, Y. Y. Yang, *Nat. Chem.* **2011**, *3*, 409 – 414; b) S. K. Samal, M. Dash, S. Van Vlierberghe, D. L. Kaplan, E. Chiellini, C. van Blitterswijk, L. Moroni, P. Dubruel, *Chem. Soc. Rev.* **2012**, *41*, 7147 – 7194; c) T. K. Nguyen, S. J. Lam, K. K. K. Ho, N. Kumar, G. G. Qiao, S. Egan, C. Boyer, E. H. H. Wong, *ACS Infect. Dis.* **2017**, *3*, 237 – 248.
[24] a) T. J. Beveridge, *J. Bacteriol.* **1999**, *181*, 4725 – 4733; b) H. Strahl, J. Errington, *Annu. Rev. Microbiol.* **2017**, *71*, 519 – 538.
[25] a) M. Perros, *Science* **2015**, *347*, 1062 – 1064; b) R. J. Melander, D. V. Zurawski, C. Melander, *MedChemComm* **2018**, *9*, 12 – 21.
[26] N. A. Turner, B. K. Sharma-Kuinkel, S. A. Maskarinec, E. M. Eichenberger, P. P. Shah, M. Carugati, T. L. Holland, V. G. Fowler, *Nat. Rev. Microbiol.* **2019**, *17*, 203 – 218.
[27] M. Zhou, Y. X. Qian, J. Y. Xie, W. J. Zhang, W. N. Jiang, X. M. Xiao, S. Chen, C. Z. Dai, Z. H. Cong, Z. M. Ji, N. Shao, L. Q. Liu, Y. Q. Wu, R. H. Liu, *Angew. Chem. Int. Ed.* **2020**, *59*, 6412 – 6419; *Angew. Chem.* **2020**, *132*, 6474 – 6481.

Manuscript received: March 22, 2021
Accepted manuscript online: April 7, 2021
Version of record online: ■■ ■■, ■■■■

Research Articles

Antibacterial Agents

J. Cheng, G. Gan, Z. Shen, L. Gao, G. Zhang, J. Hu* ———— ▮▮▮▮–▮▮▮▮

Red Light-Triggered Intracellular Carbon Monoxide Release Enables Selective Eradication of MRSA Infection

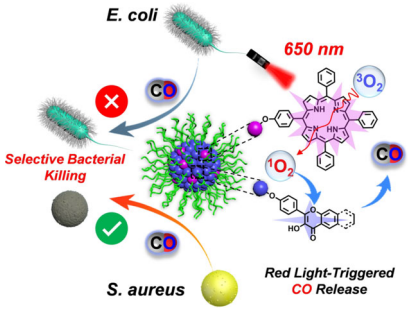

Metal-free CO-releasing micelles can be selectively taken up by Gram-positive bacteria, exerting a narrow-spectrum bactericidal activity toward only Gram-positive bacteria under red light irradiation. The CO-releasing micelles synergistically eradicate MRSA pathogens and accelerate MRSA-infected wound healing.

These are not the final page numbers!